P1A.5 RETRIEVING RAIN DROP SIZE DISTRIBUTION FROM DUAL-FREQUENCY WIND PROFILER

Eastwood Im,Li Li and Ziad S. Haddad

Jet Propulsion Laboratory, California Institute of Technology, Pasadena CA, USA

1. INTRODUCTION

Analysis of the TRMM radar data shows that, at low to moderate rain rates (2-way attenuations of up to 5 dB), the surface-reference estimates of the bulk rain (as represented by the Path Integrated Attenuation) are very poorly correlated with the a priori estimates which can be obtained from the Hitschfeld-Bordan integration of the measured radar profiles using the radar algorithm's a priori Z-k relations. This implies that, except for very high rain rates, the a priori knowledge and parametrization of radar-rain relations (hence of the drop size distributions (DSD) underlying the precipitation at TRMM and GPM resolutions) is not consistent with the TRMM radar's measurements of the sea surface. The main reason for such a discrepancy is that the available a priori DSD information comes from point-wise ground truth samples of minuscule areas, as well as the lack of information on the effect of the different surface winds within the precipitation and outside of it. In this paper, we develop and test a robust methodology to analyze wind-profiler data that can accurately quantify the 4-dimensional variability of the drop size distribution at resolutions comparable to those of the TRMM and GPM radars.

2. Objectives and Approach

The most promising approach to derive a description of the DSD that is free of the problems described above is to perform a systematic analysis of dual-frequency wind profiler data. Indeed, wind profilers are sensitive to the doppler due to turbulence as well as to the doppler signature of falling rain drops, and they sample large volumes of the atmosphere, and it is reasonable to assume that a dual-frequency profile of doppler spectra could allow one to retrieve the profile of the wind spectrum and that of the rain, i.e. the DSD. Rajopadhyaya et al (1998) have already demonstrated the merits of this idea on data gathered during the 1993-1994 wet season in Darwin, Northern Territory, Australia, at which time two wind profilers, one at VHF (50 MHz) and the other at UHF (920 MHz) were located side by side and sampling roughly the same volume overhead. The approach relies on the fact that the strong Bragg scatter due to the turbulence at 50 MHz would mask the low-fall-velocity part of the spectrum due to the rain drops. By assuming that the measured VHF spectrum is thus entirely due to the vertical wind, the spectrum s_w of the latter can be estimated using the VHF measurement, and the radar reflectivity-weighted spectrum s_R due to the DSD can subsequently be estimated from the UHF measurement s_{UHF} using the formula (see Doviak and Zrnic, 1993)

$$s_{UHF} = e_U \cdot s_w + \eta_U \cdot s_R * s_w \qquad (1)$$

in which $e_U \sim C^2 \lambda^{-1/3}$ is proportional to the refractive index structure constant C^2, and $\eta_U \sim |Kw|^2 \lambda^{-4}$ is proportional to the norm-squared of the dielectric factor of water Kw (λ is the wavelength, and s_w is assumed to have been "backed out" of the VHF spectrum). In practice, Rajopadhyaya et al. determined s_w by assuming the vertical wind was (a two-parameter) Gaussian, and fitting the mean and spread to the observed VHF spectrum s_{VHF} by a least-squares fitting of the right-hand-side of the equation

$$s_{VHF} = e_V \cdot s_w \qquad (2)$$

then assuming a Gamma DSD and determining the parameters N0, μ and Λ by performing a least-squares fit of (1). We have derived a similar method which avoids the assumption that the DSD obeys a Gamma law, and which avoids having to assume that the turbulence is Gaussian as well. We start by describing how the "Gamma" assumption (or any other analytic form) for the DSD is eliminated. We still use (1) to solve

$$\begin{aligned} s_{UHF}(v) - e_U \cdot s_w(v) &= \eta_U \cdot s_R * s_w \\ &= \eta_U \int \cdot s_R(D) \cdot s_w(v - v_0(D)) dD \end{aligned}$$

for the DSD, in the form

(3)

where v represents any doppler velocity in the spectrum, and vo(D) represents the terminal fall velocity of a drop of diameter D. Filling in the drops' reflectivity-weighted spectrum for $s_R(D)$ and combining all the constants into a single factor c gives

$$s_{UHF}(v) - e_U \cdot s_w(v) = c \int \cdot N(D) \cdot \sigma_b(D) \cdot s_w(v - v_0(D)) dD$$

(4)

There are several ways one can proceed to solve (4) for the DSD N(D). The simplest is to discretize the latter over, say, n discrete diameter bins, so that the DSD is represented by $N_1, \ldots, N_n$. Since the measured spectra are already discretized over, say, m doppler bins $v_1, \ldots, v_m$, the discretized version of (4) is a system of m equations

$$L_i = \sum_{j=1}^{n} N_j \cdot S_{ij} \qquad (5)$$

where $L_i = s_{UHF}(v_i) - e_U\, s_w(v_i)$, $S_{ij} = c\, \sigma_b(D_j) \times s_w(v_i - v_0(D)) \Delta D_j$ and i varies from 1 to m. Writing ***l*** for the vector of L_i's, **n** for the vector of N_j's, and **S** for the matrix (S_{ij}) , the problem is to solve ***l*** = **Sn** or, at least, to find an **n** so that the right-hand-side is as close as possible to the left-hand-side in the least-squares sense. This is possible as long as m, the number of observed spectrum bins, is greater than n, the number of discrete drop size bins. In that case, the least-squares solution of (5) is

$$\boldsymbol{n} = (\boldsymbol{S}^t \boldsymbol{S})^{-1} \boldsymbol{S}^t \boldsymbol{l} \qquad (6)$$

Instead of discretizing one could use some fancier smoothing window. However, we did implement the straightforward discretization described above, and the results are quite satisfactory.

Fig. 1 illustrates the result of this method on a dual-frequency doppler profile observed in Darwin on December 29, 1993. In this case, the observed spectra are discretized into m=48 doppler bins, and The DSD are discretized into 16 bins of equal width (0.4mm). The six panels on the left show the DSD spectra derived from the Γ fit (diamond) and from our binning approach (plus) corresponding to normalized wind profiler spectra measured at 1220 UTC, while the six panels on the right show the DSD spectra derived from the measurements at 1222 UTC. Fig. 2 shows the normalized doppler spectra reconstructed from the Γ-fitted estimates (dot-dashed line) and from the binned estimates (dashed line), superimposed on the actual measured spectra (solid line). Quite obviously, at every height level, the binned spectrum is much closer to the measurement than the Γ fits. These two figures also confirms that the spectra can change significantly over a two-minute time span, witness in particular the large differences at 1605m. Another example, corresponding to spectrum profiles measured on the same day at 1030 UTC, is shown in Fig. 3. Unlike the previous case, where there was a large discrepancy between the two estimated DSD's, this time the DSD's are not drastically different, yet, as Fig. 4 shows, and the binned estimate consistently produces a doppler spectrum that is much closer to the measurement, at every height level, than that reconstructed from the Γ fit.

In the examples above, the turbulence was assumed Gaussian. As Fig. 5 shows, this assumption is not entirely consistent with the observations. Figure 5 plots the measured normalized VHF spectra (solid line) and the fitted Gaussians (dotted line) corresponding to the case of Figs. 3 and 4. Evidently, the fit can overestimate the peak by up to 20% (see, for example, the spectra at 4005 and 4605m) and it fails to model any "sidelobes" (see, for example,. the spectrum at 1605m). Fortunately, it is not necessary to assume that the turbulence has a Gaussian spectrum. Indeed, we can solve for the turbulence spectrum exactly. That is because the exact spectra at the two frequencies are given by

$$s_{VHF} = e_V \cdot s_w + \eta_V \cdot s_R * s_w \qquad (7)$$

$$s_{UHF} = e_U \cdot s_w + \eta_U \cdot s_R * s_w \qquad (8)$$

One does not need to assume that the term $\eta_V\, s_R * s_w$ in (7) is negligible. In fact, after multiplying (7) by η_U and (8) by η_V, and subtracting the resulting equations, one ends up eliminating the convolution term, thus obtaining the expression

$$s_w = \frac{\eta_U \cdot s_{VHF} - \eta_V \cdot s_{UHF}}{\eta_U \cdot e_V - \eta_U \cdot e_U} \qquad (9)$$

which, since the two frequencies are well separated (i.e. the denominator of the right hand side does not vanish), determines the turbulence spectrum exactly. Once s_w is known, the binning approach can be applied exactly as before.

CONCLUSION

A methodology and algorithm have been developed to analyze wind-profiler data to accurately quantify the 4-dimensional variability of the drop size distribution at resolutions comparable to those of the TRMM and GPM radars. The new algorithm is more robust than the Γ-fit approach, and its solution always converge in the Doppler domain.

ACKNOWLEDGMENT

This research was performed at the Jet Propulsion Laboratory, California Institute of Technology under contract with the National Aeronautics and Space administration.

REFERENCES

Doviak, R.J., and Zrnic, D.S., 1993: Doppler radar and weather observations, 2nd edition, Academic Press (p. 275 for the rain doppler spectrum, p. 452 for the wind component).

Rajopadhyaya, D.K., May, P.T., Cifelli, R.C., Avery, S.K.,Willams, C.R., Ecklund,W.L., Gage, K.S., 1998: PThe effect of vertical air motions on rain rates and median volume diameter determined from combined UHF and VHF wind profiler measurements and comparisons with rain gauge measurements, J. Atmos. Ocean. Tech. 15, 1306-1319.

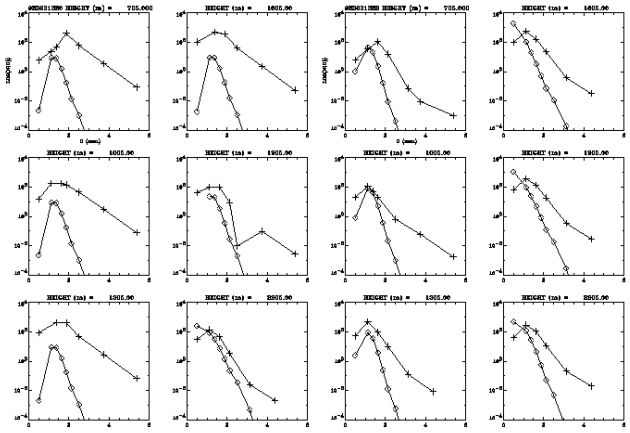

Fig. 1: N(D) verse D derived from measured spectrum. The Γ fits are represented by "◇", the binned estimates by "+".

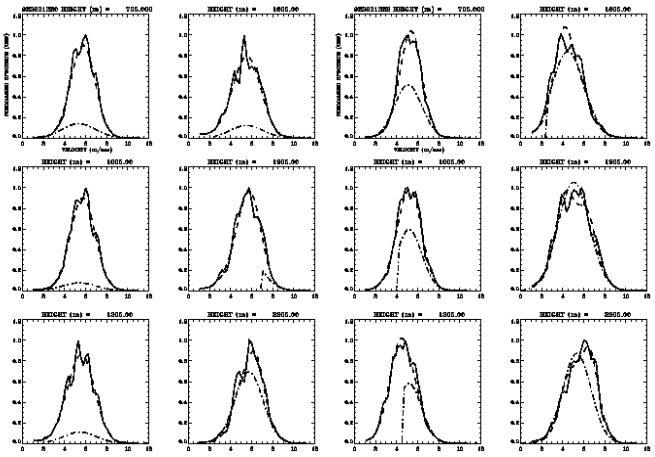

Fig. 2: Power spectral s_{UHF} verse Doppler velocity v for measured spectra (solid line), Γ-fit reconstruction (dot-dashed) and binned-estimate reconstruction (dashed) corresponding to the case of Fig. 1.

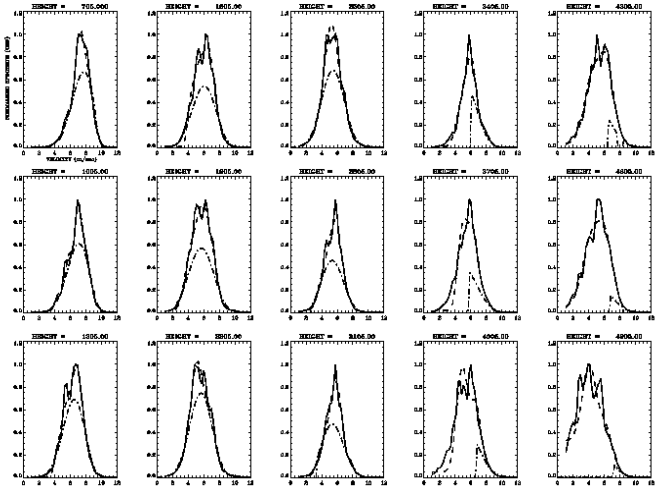

Fig. 3: N(d) verse D derived from measured spectrum profiles on 12/29/93 at 1030 UTC. The Γ fits are represented by "◇", the binned estimates by "+".

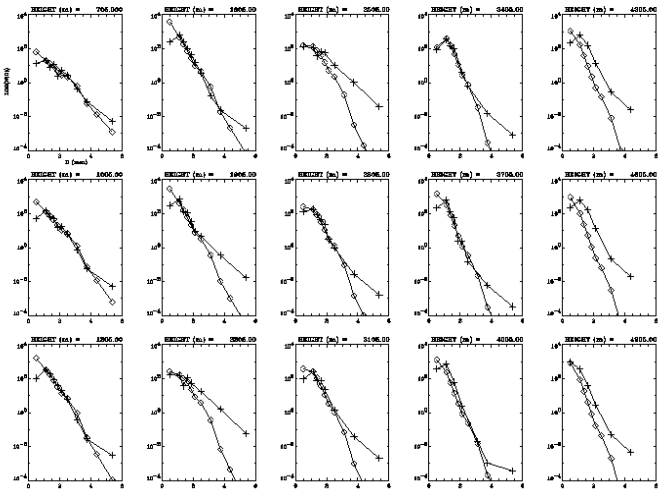

Fig. 4: Power spectral s_{UHF} verse Doppler velocity v for measured spectra (solid line), Γ-fit reconstruction (dot-dashed) and binned-estimate reconstruction (dashed) corresponding to the case of Fig. 3.

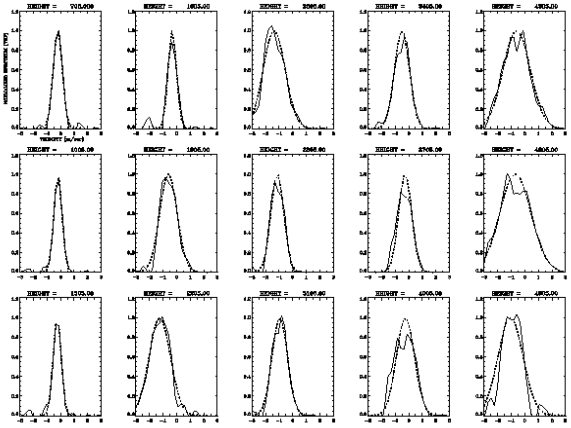

Fig. 5: Power spectral s_{VHF} verse Doppler velocity v for the case of Fig. 3, showing the measured spectrum (solid line) and the Gaussian fit (dotted line).